


## Information scrambling of the dilute Bose gas at low temperature

Chao Yin<sup>1,\*</sup> and Yu Chen<sup>2,†</sup>

<sup>1</sup>*Department of Physics and Center for Theory of Quantum Matter, University of Colorado, Boulder, Colorado 80309, USA*

<sup>2</sup>*Graduate School of China Academy of Engineering Physics, Beijing 100193, China*

 (Received 12 October 2022; revised 26 January 2023; accepted 31 January 2023; published 7 February 2023)

We calculate the quantum Lyapunov exponent  $\lambda_L$  and butterfly velocity  $v_B$  in the dilute Bose gas at temperature  $T$  deep in the Bose-Einstein condensation phase. The generalized Boltzmann equation approach is used for calculating out-of-time-ordered correlators, from which  $\lambda_L$  and  $v_B$  are extracted. At very low temperature where elementary excitations are phonon-like, we find  $\lambda_L \propto T^5$  and  $v_B \sim c$ , the sound velocity. At relatively high temperature, we have  $\lambda_L \propto T$  and  $v_B \sim c(T/T_*)^{0.23}$ . We find that  $\lambda_L$  is always comparable to the damping rate of a quasiparticle, whose energy depends suitably on  $T$ . The chaos diffusion constant  $D_L = v_B^2/\lambda_L$ , on the other hand, differs from the energy diffusion constant  $D_E$ . We find  $D_E \ll D_L$  at very low temperature and  $D_E \gg D_L$  otherwise.

DOI: [10.1103/PhysRevB.107.054503](https://doi.org/10.1103/PhysRevB.107.054503)

### I. INTRODUCTION

Butterfly effect, a defining feature for classical chaotic dynamics, also emerges in quantum settings and is crucial for understanding strongly correlated systems. To diagnose quantum chaos, the out-of-time-ordered correlator (OTOC) is first introduced by Larkin and Ovchinnikov to study disordered superconductors [1]. This idea was rarely visited until Kitaev recently revived it to understand the shock wave backaction in the black-hole scattering problem [2,3]. To be specific, we define the OTOC by two operators  $\mathcal{O}$ ,  $\tilde{\mathcal{O}}$  as

$$\mathcal{C}(t) = \text{tr}(\sqrt{\rho}[\mathcal{O}(t), \tilde{\mathcal{O}}(0)]^\dagger \sqrt{\rho}[\mathcal{O}(t), \tilde{\mathcal{O}}(0)]). \quad (1)$$

Here  $\rho = Z_\beta^{-1} e^{-\beta H}$  with  $\beta = 1/T$  as the inverse temperature, where we have set the Boltzmann constant  $k_B = 1$ , and  $Z_\beta = \text{Tr}(e^{-\beta H})$  as the partition function.  $H$  is the system Hamiltonian that evolves operators by  $\mathcal{O}(t) = e^{iHt/\hbar} \mathcal{O} e^{-iHt/\hbar}$ . For typical chaotic systems, the OTOC grows exponentially as  $\mathcal{C}(t) \sim c_0 \exp(\lambda_L t)$ , with  $c_0$  being a nonuniversal constant.  $\lambda_L$  is the quantum Lyapunov exponent that measures the growth rate of quantum chaos, which shares similarities and differences with its classical counterpart [4–6]. It was found that  $\lambda_L$  is upper-bounded by  $2\pi/\beta$  [7], and the maximal value is saturated by models with gravity duals [3,8–10], including the Sachdev-Ye-Kitaev model [11,12] dual to Jackiw-Teitelboim gravity [13–15]. Therefore, calculating  $\lambda_L$  is crucial for identifying holographic models [16–18].

More generally, an information interpretation has been discovered for OTOC [19]. Namely,  $\lambda_L$  measures how fast local information scrambles to global information, which reveals the thermalization process in a closed quantum system. Moreover, for systems with a spatial structure, if we define  $\mathcal{O}$  and  $\tilde{\mathcal{O}}$  as local operators whose locations are of distance  $r$ , then the OTOC is vanishingly small unless  $t \gtrsim r/v_B$ , for some constant  $v_B$  called the butterfly velocity [20–22].  $v_B$  can be viewed as a

$\rho$ -dependent extension [23,24] of the Lieb-Robinson velocity [25], the maximal speed information can propagate through the system. Combining  $\lambda_L$  with  $v_B$ , one can define the chaos diffusion constant  $D_L = v_B^2/\lambda_L$ . In the most chaotic systems,  $D_L$  is argued to be universally comparable with charge [21,26] and energy [27] diffusion constants.

Due to the above implications, the general properties of OTOC have raised a lot of interest (see Ref. [28] for a recent review). For example, OTOC has been theoretically calculated in many-body-localized systems [29–33], integrable systems [34], and diffusive metals [35–37], and experimentally measured in NMR systems [38–40], ion traps [41,42], and superconducting circuits [43–45]. However, OTOC remains to be studied for the dilute Bose gas in Bose-Einstein condensation (BEC), realizable in cold atom experiments [46]. Moreover, unlike models studied before, BEC hosts two temperature regimes with qualitatively different elementary excitations. How does information scramble in the crossover temperature regime? In this paper, we fill this gap by using the generalized Boltzmann equations (GBE) approach [47–50].

The rest of the paper is structured as follows: In Sec. II, our model is introduced, where we focus on the BEC regime  $T \ll T_{\text{BEC}}$ . We identify a crossover temperature  $T_* \ll T_{\text{BEC}}$ , where quasiparticle excitations change from phonon-like at  $T \ll T_*$  to particle-like at  $T \gg T_*$ . In Sec. III, we apply the augmented Keldysh formalism to derive GBE that govern the evolution of OTOC, to the leading nontrivial order of the interaction strength  $g$ . In Section IV, we extract  $\lambda_L$  from the GBEs for the whole temperature regime  $T \ll T_{\text{BEC}}$  and get  $\lambda_L \propto T^5$  for  $T \ll T_*$  and  $\lambda_L \propto T$  for  $T \gg T_*$ . We further show that  $\lambda_L$  is comparable to the damping rate of a quasiparticle at a suitably defined energy, which can be extracted from traditional Boltzmann equations. In Sec. V, we present our results on  $v_B$ . It is of the order of the sound velocity  $c$  at  $T \ll T_*$  and grows as a power law  $v_B \sim T^{0.23}$  for  $T \gg T_*$ . We further show that for both temperature regimes, the chaos diffusion constant  $D_L$  and the energy diffusion constant  $D_E$  are not related to each other. We finally conclude in Sec. VI.

\*chao.yin@colorado.edu

†ychen@gcsaep.ac.cn

## II. MODEL

Here we introduce our model. Consider  $N$  bosons contained in a three-dimensional box of volume  $V = L^3$ . Using  $\psi(\mathbf{x})$  to be the complex field operator that annihilates a boson at space position  $\mathbf{x}$ , we study the homogeneous Bose gas with Hamiltonian

$$H_{\text{BG}} = H_K + H_V, \quad (2)$$

where the kinetic energy is

$$H_K = \int d\mathbf{x} \psi^\dagger(\mathbf{x}) \left( -\frac{\hbar^2}{2m} \nabla^2 \right) \psi(\mathbf{x}), \quad (3)$$

with  $m$  being the boson mass. The interaction  $H_V$  is given by

$$H_V = \frac{g}{2} \int d\mathbf{x} \psi^\dagger(\mathbf{x}) \psi^\dagger(\mathbf{x}) \psi(\mathbf{x}) \psi(\mathbf{x}), \quad (4)$$

where we have assumed the temperature is sufficiently low, so that pairs of bosons feel a  $\delta$  function pseudopotential [51]

$$v(\mathbf{x} - \mathbf{x}') = \frac{4\pi a_s \hbar^2}{m} \delta(\mathbf{x} - \mathbf{x}') \equiv g\delta(\mathbf{x} - \mathbf{x}'), \quad (5)$$

determined by the  $s$ -wave scattering length  $a_s$  (or equivalently, the interaction strength  $g$ ). In the momentum space, we define the boson annihilation operator at wave vector  $\mathbf{k}$  by  $a_{\mathbf{k}} = V^{-1} \int d\mathbf{x} \psi(\mathbf{x}) e^{-i\mathbf{k}\cdot\mathbf{x}}$ . Then  $H_{\text{BG}}$  can be rewritten as

$$H_{\text{BG}} = \sum_{\mathbf{k}} \epsilon_{\mathbf{k}} a_{\mathbf{k}}^\dagger a_{\mathbf{k}} + \frac{g}{2V} \sum_{\mathbf{k}_1, \mathbf{k}_2, \mathbf{k}_3} a_{\mathbf{k}_1}^\dagger a_{\mathbf{k}_2}^\dagger a_{\mathbf{k}_3} a_{\mathbf{k}_1 + \mathbf{k}_2 - \mathbf{k}_3}, \quad (6)$$

where  $\epsilon_{\mathbf{k}} = \hbar^2 k^2 / 2m$ ,  $k = |\mathbf{k}|$ , and  $\mathbf{k}$  takes values in  $\{2\pi n/L : n \in \mathbb{Z}^3\}$ .

There are three independent length scales in this model: the scattering length  $a_s$ , the interparticle spacing  $n^{-1/3}$  where  $n = N/V$ , and the thermal wavelength

$$\lambda_T = \sqrt{\frac{2\pi \hbar^2}{mT}}. \quad (7)$$

We focus on the dilute and low-temperature limit

$$na_s^3 \ll 1, \quad n\lambda_T^3 \gg 1, \quad (8)$$

where perturbation theory applies. In this regime close to equilibrium, nearly all  $N$  bosons condense in the zero-momentum state, forming a BEC [51]. As in standard Bogoliubov theory for a homogeneous BEC, we approximate the zero-momentum creation and annihilation operators in (6) by a large  $c$  number  $\sqrt{N_0} \approx \sqrt{N}$ :

$$a_0 = a_0^\dagger = \sqrt{N}, \quad (9)$$

where we have ignored higher-order corrections  $N - N_0 \propto (na_s^3)^{1/2}$  [51]. Moreover, we use the standard Bogoliubov transformation to obtain the effective Hamiltonian from (6):

$$H = H_0 + H_1, \quad \text{where} \quad (10a)$$

$$H_0 = \sum_{\mathbf{k}} \mathcal{E}_{\mathbf{k}} \alpha_{\mathbf{k}}^\dagger \alpha_{\mathbf{k}} \quad \text{and} \quad (10b)$$

$$H_1 = \frac{g}{\sqrt{V}} \sum_{\mathbf{k}_1, \mathbf{k}_2} M_{\mathbf{k}_1, \mathbf{k}_2} (\alpha_{\mathbf{k}_1}^\dagger \alpha_{\mathbf{k}_2}^\dagger \alpha_{\mathbf{k}_1 + \mathbf{k}_2} + \text{H.c.}), \quad (10c)$$

where  $\alpha_{\mathbf{k}}$  and  $\alpha_{\mathbf{k}}^\dagger$  are the annihilation and creation operators for the Bogoliubov quasiparticle, with boson commutation relation

$$[\alpha_{\mathbf{k}}, \alpha_{\mathbf{k}'}^\dagger] = \delta_{\mathbf{k}, \mathbf{k}'}. \quad (11)$$

In (10), the quasiparticle has spectrum

$$\mathcal{E}_{\mathbf{k}} = \sqrt{\epsilon_{\mathbf{k}}(\epsilon_{\mathbf{k}} + 2gn)}, \quad (12)$$

and collision matrix [52]

$$M_{\mathbf{k}_1, \mathbf{k}_2} = \sqrt{n} \frac{\mathbf{E}_1 + \mathbf{E}_2 - \mathbf{E}_3 + 3\mathbf{E}_1 \mathbf{E}_2 \mathbf{E}_3}{4\sqrt{\mathbf{E}_1 \mathbf{E}_2 \mathbf{E}_3}}, \quad (13)$$

with  $\mathbf{E}_i \equiv \epsilon_{\mathbf{k}_i} / \mathcal{E}_{\mathbf{k}_i}$  and  $\mathbf{k}_3 = \mathbf{k}_1 + \mathbf{k}_2$ . In deriving (10), we have discarded a  $c$ -number term, and higher-order terms in  $1/N$ . We have also discarded the term  $\propto \alpha_{\mathbf{k}_1} \alpha_{\mathbf{k}_2} \alpha_{-\mathbf{k}_1 - \mathbf{k}_2} + \text{H.c.}$ , which describes the process that creates or annihilates three quasiparticles simultaneously. At leading order, such off-shell processes do not contribute to the kinetic equations that we will derive. Equation (10) is then our starting point for a field-theoretic calculation for information scrambling, and in the end of Sec. III we will justify the Bogoliubov approximation (9) in this nonequilibrium context. Note that, although strictly speaking, the sums over  $\mathbf{k}$  in (10) should avoid the  $\mathbf{k} = \mathbf{0}$  point, this makes no difference for latter calculations, since  $\mathcal{E}_{\mathbf{k}}$  and  $M_{\mathbf{k}_1, \mathbf{k}_2}$  both become zero when one of the  $\mathbf{k}$  arguments (including  $\mathbf{k}_3$ ) is set to  $\mathbf{0}$ .

Equation (12) suggests a crossover behavior for the quasiparticles. Defining the characteristic momentum  $k_0 \equiv \sqrt{mgn}/\hbar = \sqrt{4\pi a_s n}$ , the quasiparticles change from phonon-like  $\mathcal{E}_{\mathbf{k}} \approx \hbar c k$  at  $k \ll k_0$ , where the sound velocity  $c = \sqrt{gn/m}$ , to particle-like  $\mathcal{E}_{\mathbf{k}} \approx \epsilon_{\mathbf{k}}$  at  $k \gg k_0$ . The corresponding crossover temperature is  $T_* \equiv \hbar^2 k_0^2 / m = \hbar c k_0 = gn$ . Thus we expect that OTOC also behaves differently at the two temperature regimes: very low temperature  $T \ll T_*$ , and relatively high temperature  $T_* \ll T \ll T_{\text{BEC}}$ .

## III. THE AUGMENTED KELDYSH FORMALISM

In this section we set  $\hbar = 1$ . We first remark on our regularization in (1), namely, inserting two  $\sqrt{\rho}$  between the commutators. The advantage is threefold: It avoids potential ultraviolet divergences and is the one for which the chaos bound [7] is proved. Moreover, in kinetic theory it has a clear physical meaning related to classical chaos [53].

Equation (1) contains four terms that can be arranged as

$$\mathcal{C}(t) = 2 \text{Re} \tilde{\mathcal{C}}(t) + \text{TOCs}, \quad \text{where}$$

$$\tilde{\mathcal{C}}(t) = \text{tr}(\sqrt{\rho} \mathcal{O}(t) \tilde{\mathcal{O}}(0) \sqrt{\rho} \mathcal{O}(t) \tilde{\mathcal{O}}(0)). \quad (14)$$

Here TOCs stands for time-ordered correlations, and we have assumed the operators to be Hermitian for simplicity. We focus on  $\tilde{\mathcal{C}}(t)$  because TOCs do not host exponential growth.

### A. Relation between OTOC and TOC in a doubled system

To calculate OTOC in (14), we first introduce the time contour  $C$  shown on the left of Fig. 1, which contains two parts: up( $u$ ) and down( $d$ ), with each part containing two branches: for example  $u$  contains  $u+$  and  $u-$ . Such  $C$  is called the augmented Keldysh contour introduced in Ref. [47]: if there is

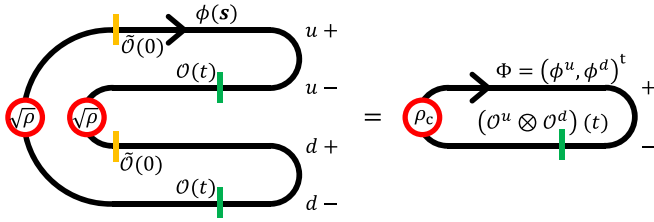


FIG. 1. The augmented Keldysh contour  $C$  (left) for OTOC in (1) is equivalent to the conventional Keldysh contour  $C_c$  (right), where the fields are doubled, and the initial state  $\rho_c$  includes the perturbation from  $\tilde{\mathcal{O}}$ .

only one part (up or down) instead, then it is the conventional Keldysh contour [54] that is used for calculating TOC. We parametrize  $C$  by the contour time  $s$ , which goes from  $t = 0^-$  (the time slightly before 0) to  $t = +\infty$  and back to  $t = 0^-$  in the up part of  $C$ , and then goes to  $+\infty$  and back to  $0^-$  again in the down part of  $C$ , completing one cycle of the whole contour. Equivalently one can describe the contour time by the doublet  $s = (\kappa, t)$ , where the Keldysh label  $\kappa = u+, u-, d+, d-$  denotes the branch that the conventional time  $t \in (0^-, +\infty)$  lives in. Define the contour Hamiltonian  $H(s)$

$$H(s) = \begin{cases} H - \frac{i}{2}\beta H\delta(t+0), & \kappa = u+, d+ \\ -H, & \kappa = u-, d-, \end{cases} \quad (15)$$

where the  $\delta$  function at  $(u+, 0^-)$  and  $(d+, 0^-)$  accounts for the thermal density matrix  $\rho$ . Then (14) can be rewritten on this contour  $C$ :

$$\begin{aligned} \tilde{\mathcal{C}}(t) &= \langle \mathcal{T}_C \mathcal{O}_{d-}(t) \tilde{\mathcal{O}}_{d+}(0) \mathcal{O}_{u-}(t) \tilde{\mathcal{O}}_{u+}(0) e^{-i \int_C ds H(s)} \rangle \\ &= \int [D\phi] \mathcal{O}_{d-}(t) \tilde{\mathcal{O}}_{d+}(0) \mathcal{O}_{u-}(t) \tilde{\mathcal{O}}_{u+}(0) e^{iS[\phi]}, \end{aligned} \quad (16)$$

where in the first line,  $\mathcal{T}_C$  time orders the operators by its position in the contour  $C$ , and  $\langle \cdot \rangle = Z_\beta^{-1} \text{Tr}(\cdot)$ . In the second line we used the path integral representation by replacing operators  $\alpha_k$  and  $\alpha_k^\dagger$  with classical fields  $\phi_k(s)$  and  $\bar{\phi}_k(s)$  that live on the contour  $C$ , and defined the contour action

$$S[\phi] = S_0[\phi] + S_1[\phi], \quad (17)$$

where  $S_0$  and  $S_1$  correspond to  $H_0$  and  $H_1$  in (10), respectively, whose expressions are given later. We now provide several remarks on (16). First, the Keldysh  $\kappa$  labels are not unique because the operator insertions can move along the contour:  $\mathcal{O}_{u-}(t)$  can be replaced by  $\mathcal{O}_{u+}(t)$  for example. Second, for notational simplicity we omit the functional dependence of  $S$  on  $\bar{\phi}$ , which is also integrated in  $\int [D\phi]$ . Lastly, we use  $\mathcal{O}_\kappa(t)$  for both the quantum operator  $\mathcal{O}$  at  $s = (\kappa, t)$ , and its path integral representation that is a function of  $\phi(s)$  and its time derivatives.

We have expressed (14) as a path integral along the augmented Keldysh contour  $C$ , which gets rid of operators and their time ordering. As a result, there is an equivalent perspective that turns out to be useful: The path integral can be viewed as one along a *conventional* Keldysh contour  $C_c$  as shown on the right of Fig. 1 instead, by merging the up and down parts of  $C$ , so that there are two sets of fields  $\phi^u(s)$  and  $\phi^d(s)$  that live on the contour  $C_c$ . Here  $s$  is the contour time for  $C_c$ , and

we combine the fields to a two-component one  $\Phi = (\phi^u, \phi^d)^t$  with its conjugate  $\bar{\Phi} = (\bar{\phi}^u, \bar{\phi}^d)$ . The operator insertions are also combined, where the initial perturbations  $\tilde{\mathcal{O}}$  are absorbed into the initial state  $\rho_c$ . Later we find the specific form of  $\mathcal{O}$ ,  $\tilde{\mathcal{O}}$ , and  $\rho_c$  is irrelevant for us to extract  $\lambda_L$  and  $\nu_B$ . The action governing the contour evolution in  $0 < t < \infty$  factorizes to up and down contributions, so that the OTOC is converted to a TOC  $\langle \mathcal{O}_{u-}(t) \mathcal{O}_{d-}(t) \rangle$ , for a doubled system: the original one,  $u$ , together with its augmented ancilla system  $d$ . Here we call  $\langle \mathcal{O}_{u-}(t) \mathcal{O}_{d-}(t) \rangle$  a TOC because it can be calculated on a single Keldysh contour. To be more precise, it can be viewed as  $\langle (\mathcal{O} \otimes \mathcal{O})(t) I(0) \rangle$ , where the two  $\mathcal{O}$  are combined to one operator  $\mathcal{O} \otimes \mathcal{O}$ , and an identity operator is inserted at time 0 to make the time order manifest. The two subsystems have the same Hamiltonian (10) for time evolution and do not couple to each other. However, there is a price to pay: The initial state  $\rho_c$ , for the average  $\langle \cdot \rangle$  appearing in the TOC, includes the perturbation  $\tilde{\mathcal{O}}$  and becomes a complicated entangled state shared by the two subsystems, which is expressed pictorially in Fig. 1. (Without the perturbation, the density matrix for each subsystem is the exact thermal state  $\rho$ , because tracing  $d$ , for example, is equivalent to removing the two operators  $\tilde{\mathcal{O}}(0)$ ,  $\mathcal{O}(t)$  in the  $d$  part of the left of Fig. 1, so that the two  $\sqrt{\rho}$  insertions combine to one  $\rho$  as the initial state of  $u$ .) This perturbed initial entangled state leads to correlations shared by the two subsystems, and the growth of  $\mathcal{C}(t)$  measures how such correlations, probed by the local operator  $\mathcal{O}$ , decay when evolving from the initial state  $\rho_c$ . At long times  $\mathcal{C}(t)$  stays at some large value, which means the two subsystems have *locally* forgotten about the initial condition and become uncorrelated [47].

## B. Overview of the derivation

With the above relation to TOC in the doubled system  $u + d$ , it is transparent that conventional Keldysh techniques (see Ref. [54] for a pedagogical review) apply here with slight modifications. Here we sketch the idea before diving into technical details.

Without interaction, the problem is solvable by explicit single-particle Green's function  $G_0$ , which contains three exponents: “retarded”  $G_0^R$ , “advanced”  $G_0^A$ , and “Keldysh”  $G_0^K$ . With interaction, the full Green's function  $G$  is related to  $G_0$  via the self-energy  $\Sigma$  in the Dyson equation (28), and some approximation needs to be made.

First, we take the semiclassical approximation so that the Dyson equation for  $G^K$  amounts to a kinetic Boltzmann equation for some quasiparticle distribution function  $F(t, \mathbf{x}, \mathbf{k})$ , whose initial value is determined by  $\rho_c$ . This requires that the initial state  $\rho_c$ , perturbed by  $\tilde{\mathcal{O}}$ , fluctuates in length scales much larger than the microscopic ones.

Second, since the interaction is weak, we take the self-consistent Born approximation [54] for  $\Sigma$ , namely, setting  $G^R$ ,  $G^A$  to their noninteracting counterparts while keeping the full  $G^K$  expressed by  $F$ . This leads to *nonlinear* partial differential equations for  $F$ , the GBEs. It is argued that considering further contributions beyond this approximation does not change the form of the resulting GBE [47] because it merely changes the spectrum and interaction vertex in a nonqualitative way.

Third, we linearize the GBE by assuming there is a time window in which  $F$  is close to its unstable fixed point  $F_0$  of the GBE, which turns out to be the value without interaction and operator perturbation. Since the expectation of a general local operator  $\mathcal{O}$  is a function of the distribution  $F$ , we find  $\lambda_L, v_B$  simply by extracting the fastest growing mode  $F - F_0 \sim e^{\lambda_L(t-x/v_B)}$  from the GBE on how  $F$  deviates from  $F_0$ . The result then does not depend on the specific form of  $\mathcal{O}$ , and the initial state  $\rho_c$  that includes the interacting density matrix  $\rho$  and  $\tilde{\mathcal{O}}$ . We only require that  $\rho$  is close to the noninteracting  $\rho_0$ , and that  $\tilde{\mathcal{O}}$  is weakly perturbing and “smeared out” (justifying our first approximation above). As another perspective,  $\rho$  becomes irrelevant by arguing that it can be viewed as the state evolved from the noninteracting  $\rho_0$  in the far past  $t = -\infty$ , with interaction adiabatically turned on [54].

### C. Keldysh rotation

We first focus on the noninteracting case in this section to motivate such techniques, which also provides building blocks for the interacting case. The noninteracting action on contour  $C_c$  is

$$S_0[\Phi] = \int dt \sum_{s=\pm} \sum_k s \bar{\Phi}_k^s(t) (i\partial_t - \mathcal{E}_k) \Phi_k^s(t), \quad (18)$$

where the kernel  $i\partial_t - \mathcal{E}_k$  should be understood as a diagonal matrix acting on the  $(u, d)$  space.  $s = \pm$  is the branch index, + for forward time evolution and - for backward. Despite of the factorized form of  $S_0$ , the two sets of fields  $\Phi^+$  and  $\Phi^-$  are correlated because the two branches are connected at  $t = 0$  and  $t = \infty$ . The connection at  $t = \infty$  is a trivial continuity condition, while that at  $t = 0$  involves inserting the initial state  $\rho_c$ . Due to these connections, the Green’s functions  $\langle \Phi^s(t) \bar{\Phi}^{s'}(t') \rangle_0$  satisfy exact causality conditions. For example, for  $t' > t$  we have  $\langle \Phi(t)^+ \bar{\Phi}^+(t') \rangle_0 = \langle \Phi(t)^+ \bar{\Phi}^-(t') \rangle_0$  by moving  $\bar{\Phi}^+$  from  $t'$  along the contour to  $\infty$  and then back to  $t'$ , with the field becoming  $\bar{\Phi}^-$ . To make such conditions manifest, we pursue the Keldysh rotation [54]:

$$\begin{pmatrix} \Phi^1(t) \\ \Phi^2(t) \end{pmatrix} = \frac{1}{\sqrt{2}} \begin{pmatrix} 1 & 1 \\ 1 & -1 \end{pmatrix} \begin{pmatrix} \Phi^+(t) \\ \Phi^-(t) \end{pmatrix}, \quad (19)$$

where  $\Phi^1$  and  $\Phi^2$  are often referred to as the “classical” and “quantum” field, respectively. The new fields have Green’s functions of the form

$$\langle \Phi^s(t) \bar{\Phi}^{s'}(t') \rangle_0 \equiv iG_0^{ss'}(t, t') = i \begin{pmatrix} G_0^K(t, t') & G_0^R(t, t') \\ G_0^A(t, t') & 0 \end{pmatrix}, \quad (20)$$

where  $K, R, A$  stand for “Keldysh,” “retarded,” and “advanced,” and the zero matrix element is due to causality. Here index  $s = 1, 2$  is introduced to label the degrees of freedoms in the retard-advanced (RA) space. Recall that  $G_0^K, G_0^R, G_0^A$  are themselves matrices in the  $(u, d)$  space:

$$G_0^K = \begin{pmatrix} G_0^{Kuu} & G_0^{Kud} \\ G_0^{Kdu} & G_0^{Kdd} \end{pmatrix}, \quad G_0^{R/A} = \begin{pmatrix} G_0^{R/Auu} & 0 \\ 0 & G_0^{R/Add} \end{pmatrix}. \quad (21)$$

Thus the Green’s functions can be labeled as  $G^{\kappa\kappa'} = G^{ss',\sigma\sigma'}$ , where  $\sigma = u (d)$  is introduced for the up (down) index. One can also notice that  $G^{R/Auu} = G^{R/Add}$  due to causality [47]. In the absence of the initial perturbation  $\tilde{\mathcal{O}}$ , the system is in equilibrium so that the Green’s functions only depend on the time difference  $\bar{G}_0^{\kappa\kappa'}(t, t') = \bar{G}_0^{\kappa\kappa'}(t - t')$ , with the symbol  $\bar{\cdot}$  denoting equilibrium. Then  $\bar{G}_0$  can be Fourier transformed to frequency space,  $\bar{G}_0^{\kappa\kappa'}(\omega) = \int dt \bar{G}_0^{\kappa\kappa'}(t) e^{i\omega t}$ . From the specific form of  $\rho_c$  without the perturbation, one can derive [47,54]

$$G_{0,k}^{R/Auu}(\omega) = G_{0,k}^{R/Add}(\omega) = G_0^{R/A}(\omega) = (\omega - \mathcal{E}_k \pm i0)^{-1}, \quad (22a)$$

$$\bar{G}_{0,k}^{Kuu}(\omega) = \bar{G}_{0,k}^{Kdd}(\omega) = -2\pi i \coth\left(\frac{\omega}{2T}\right) \delta(\omega - \mathcal{E}_k), \quad (22b)$$

$$\bar{G}_{0,k}^{Kdu}(\omega) = \bar{G}_{0,k}^{Kud}(\omega) = -2\pi i \left[ \sinh\left(\frac{\omega}{2T}\right) \right]^{-1} \delta(\omega - \mathcal{E}_k). \quad (22c)$$

Here we use  $G_0^{R/A}$  instead of  $\bar{G}_0^{R/A}$  because of the noninteracting nature that retarded or advanced Green functions do not depend on the initial state [54]: For example, (26) holds even when the perturbation  $\tilde{\mathcal{O}}$  is present. The up and down diagonal elements of  $\bar{G}_0$  agree with the conventional Keldysh result, since the initial density matrix for each subsystem is just  $\rho$ . In particular, these Green’s functions satisfy the fluctuation-dissipation theorem (FDT):

$$\bar{G}_0^{Kuu}(\omega) = F_0(\omega) [G_0^R(\omega) - G_0^A(\omega)], \quad \text{where} \\ F_0(\omega) = \coth\left(\frac{\omega}{2T}\right). \quad (23)$$

Similarly, one can write down the generalized version of FDT for the off-diagonal element, where the two subsystems are jointly probed by the fields:

$$\bar{G}_0^{Kdu}(\omega) = F_0^{du}(\omega) [G_0^R(\omega) - G_0^A(\omega)], \quad \text{where} \\ F_0^{du}(\omega) = \left[ \sinh\left(\frac{\omega}{2T}\right) \right]^{-1}. \quad (24)$$

### D. The generalized Boltzmann equations

Having formalized the noninteracting theory for  $H_0$ , we treat  $H_1 \propto g$  perturbatively and calculate the full Green’s function  $G^{ss'}(t, t') = -i \langle \Phi^s(t) \bar{\Phi}^{s'}(t') \rangle$  to second order of  $g$ . To this end, we first note that  $G$  can be written in the form of (20) and (21), with all zeros removed in subscripts, because  $G$  obey the same causality conditions as  $G_0$ . We start with writing down the interaction action from (10c),

$$S_1[\phi] = \frac{-g}{\sqrt{2V}} \int dt \sum_{\sigma=u,d} \sum_{\mathbf{k}_1, \mathbf{k}_2} (\bar{\phi}_1^{\sigma 1} \bar{\phi}_2^{\sigma 1} \phi_3^{\sigma 2} + 2\bar{\phi}_1^{\sigma 1} \bar{\phi}_2^{\sigma 2} \phi_3^{\sigma 1} + \bar{\phi}_1^{\sigma 2} \bar{\phi}_2^{\sigma 2} \phi_3^{\sigma 1} + \text{c.c.}), \quad (25)$$

where the Keldysh rotation has been performed, and  $\phi_j$  is the shorthand notation for  $\phi_{k_j}$ , with  $\mathbf{k}_3 = \mathbf{k}_1 + \mathbf{k}_2$  being implicit. Expanding the path integral in powers of  $g$ , we calculate the



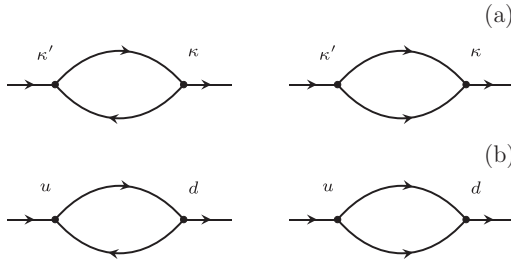


FIG. 2. Feynman diagrams for the self-energy (a)  $-i\Sigma^{\kappa\kappa'}$ , and in particular, (b)  $-i\Sigma^{Kdu}$ . (a) The Keldysh labels  $\kappa, \kappa'$  are in RA and  $ud$  space. The first Feynman diagram can be viewed as a virtual Landau damping followed by a Belieav damping. The second diagram can be viewed as a virtual Belieav damping followed by a Landau damping process. (b)  $-i\Sigma^{Kdu}$  as a special case of panel (a). The up and down indexes are denoted at the vertices, since  $u$  and  $d$  do not mix by the interaction (25). Furthermore, the internal lines only involve  $G^{Kud}$  and  $G^{Kdu}$  due to the RA structure in (25), and no spin index is summed over.

self-energy

$$\Sigma = \begin{pmatrix} 0 & \Sigma^A \\ \Sigma^R & \Sigma^K \end{pmatrix}, \quad (26)$$

which corresponds to the one-particle irreducible diagrams for the Green's function. When expanded to the up-down basis, we have

$$\Sigma^K = \begin{pmatrix} \Sigma^{Kuu} & \Sigma^{Kud} \\ \Sigma^{Kdu} & \Sigma^{Kdd} \end{pmatrix}, \quad \Sigma^{R/A} = \begin{pmatrix} \Sigma^{R/A} & 0 \\ 0 & \Sigma^{R/A} \end{pmatrix}, \quad (27)$$

whose corresponding Feynman diagrams are summarized in Fig. 2 for the leading order  $\approx g^2$ . The self-energy  $\Sigma$  is related to the full Green's function by the Dyson equation

$$(\hat{G}_0^{-1} - \hat{\Sigma}) \circ \hat{G} = \hat{1}, \quad (28)$$

where the hat symbol  $\hat{A}$  means that  $A$  is viewed as a matrix acting on the direct product space of the momentum-frequency space (which is suitably discretized), and the four-dimensional augmented Keldysh space. The symbol  $\circ$  means the matrix multiplication on this direct product space, which involves the convolution in the continuous space-time. Eq. (28) can be rewritten as  $\hat{\Sigma} = \hat{G}_0^{-1} - \hat{G}^{-1}$ , so that the causality structure of  $G$  and  $G_0$  gives rise to the structure of  $\Sigma$  in (26) and (27).

Motivated by (23) and (24), we introduce the Hermitian distribution matrix  $\hat{F}$  to encode the initial condition at  $t = 0$ :

$$\hat{G}^K = \hat{G}^R \circ \hat{F} - \hat{F} \circ \hat{G}^A, \quad (29)$$

Plugging this parametrization into the Dyson equation (28), we get

$$(\hat{G}_0^R)^{-1} \circ \hat{F} - \hat{F} \circ (\hat{G}_0^A)^{-1} = \hat{\Sigma}^R \circ \hat{F} - \hat{F} \circ \hat{\Sigma}^A - \hat{\Sigma}^K, \quad (30)$$

where we have discarded a term  $\hat{G}_0^{K-1}$  that is infinitesimal due to (22a). The kinetic equation (30) is formally exact, and determines the evolution of  $F$  if  $\Sigma$  is expressed as a functional of  $F$  in a self-consistent way, as we will show in the next section.

However, (30) is difficult to solve in general. To get a semiclassical Boltzmann-like version from (30), we take the standard assumption [54] that the dynamics perturbed from

equilibrium varies slowly in space and time, compared with the microscopic scales. Then for any two point function such as the distribution function  $F(x_1, x_2) = F(\mathbf{x}_1, t_1, \mathbf{x}_2, t_2)$ , we perform the Wigner transformation

$$F(x, p) = \int dx' e^{-ipx'} F\left(x + \frac{x'}{2}, x - \frac{x'}{2}\right), \quad (31)$$

where  $p = (\omega, \mathbf{k})$  and  $px' \equiv \mathbf{k} \cdot \mathbf{x}' - \omega t'$ . Assuming such functions vary slowly with  $x$ , one can expand the convolution in their derivatives. For example,  $\hat{\Sigma}^R \circ \hat{F}$  is Wigner transformed to

$$\begin{aligned} (\Sigma^R F)(x, p) &\approx \Sigma^R(x, p) F(x, p) \\ &+ \frac{i}{2} (\partial_x \Sigma^R \partial_p F - \partial_p \Sigma^R \partial_x F), \end{aligned} \quad (32)$$

with the arguments  $(x, p)$  being implicit in the second line. Furthermore, since to leading order  $F(x, p)$  always appear with

$$G_0^{Ruu/dd}(p) - G_0^{Auu/dd}(p) = -2\pi i \delta(\omega - \mathcal{E}_k), \quad (33)$$

according to (29), we can set the argument  $\omega$  of  $F(x, \mathbf{k}, \omega)$  on-shell:

$$F(x, \mathbf{k}, \mathcal{E}_k) \rightarrow F(x, \mathbf{k}), \quad (34)$$

so that the reduced distribution  $F(x, \mathbf{k})$  is interpreted semiclassically as the quasiparticle distribution function at time  $t$ , position  $\mathbf{x}$ , and momentum  $\mathbf{k}$ . Using the above two approximations, i.e., derivative expansion and on-shell approximation, (30) becomes the GBE:

$$[(Z')^{-1} \partial_t + \mathbf{v}'_k \cdot \nabla_x - (\nabla_x \text{Re} \Sigma^R) \cdot \nabla_k] F = \text{St}[F], \quad (35)$$

where

$$(Z')^{-1} = 1 - \partial_\omega \text{Re} \Sigma^R, \quad \mathbf{v}'_k = \nabla_k (\mathcal{E}_k + \text{Re} \Sigma^R), \quad (36)$$

and the collision integral

$$\text{St}[F] = (i\Sigma^K + 2F \text{Im} \Sigma^R)|_{\omega=\mathcal{E}_k}. \quad (37)$$

Here we have used  $\Sigma^A = (\Sigma^R)^*$ . From now on, we work with leading order of the interaction strength  $g$ . Then the terms  $\propto \text{Re} \Sigma^R$  on the left-hand side of (35) can be ignored, since the spatial and time derivatives are already small in  $g$  according to the right-hand side.

### E. Self-energy calculation

In this section we express the self-energy  $\Sigma(x, p)$  using the distribution function  $F(x, p)$ , so that (35) becomes a closed dynamical equation of  $F$ . In the spirit of the derivative expansion above,  $\Sigma(x, p)$  only depends on the local  $F(x, p')$  at the same space-time  $x$ , so we ignore the  $x$  label below. The Feynman diagrams at leading order  $\Sigma \sim g^2$  are shown in Fig. 2(a), where the Keldysh labels  $\kappa, \kappa'$  are viewed as spin indices. The internal propagators involve all three types of Green's function in (20). We set the retarded and advanced propagators to be the bare  $G_0^{R/A}$  in (22a), which do not depend on the initial state. In contrast, we set the Keldysh propagators to be the nonperturbative  $G^K$  that depends on  $F$  via (29), in which  $\hat{G}^R$  and  $\hat{G}^A$  are again replaced by its bare counterpart. In this way we self-consistently “resum” the contributions from

the nonequilibrium distribution  $F$ , while keeping the spectral Green's functions  $G^{R/A}$  at leading orders. This resummation will lead to *nonlinear* partial differential equations for  $F$ .

As an explicit example, we derive the off-diagonal self-energy  $\Sigma^{Kdu}$  in detail. The Feynman diagrams for  $\Sigma^{Kdu}$  are shown in Fig. 2(b), which only involve  $G^{Kud}$  and  $G^{Kdu}$  as internal propagators. For the left diagram in Fig. 2(b), the two internal lines are  $iG^{Kdu}(q)$  and  $iG^{Kud}(p+q)$  with  $p = (\omega, \mathbf{k})$  and  $q = (q_0, \mathbf{q})$  being the external and loop four-momentum. The vertices correspond to the second term in the bracket in (25) and its complex conjugate, which contribute a factor  $(\frac{-2ig}{\sqrt{2V}}M_{\mathbf{k},\mathbf{q}})^2$ . Finally, we sum over momentum  $\mathbf{q}$  and integrate over frequency  $\int \frac{dq_0}{2\pi}$  to get the contribution from the left

diagram,

$$\begin{aligned} & -i\Sigma_{\text{L}}^{Kdu}(p) \\ & = 2g^2 \int \frac{d^4q}{(2\pi)^4} M_{\mathbf{k},\mathbf{q}}^2 G^{Kdu}(q) G^{Kud}(p+q), \\ & = -2g^2 \int \frac{d^3\mathbf{q}}{(2\pi)^2} M_{\mathbf{k},\mathbf{q}}^2 F_{\mathbf{q}}^{du} F_{\mathbf{k}+\mathbf{q}}^{du} \delta(\omega + \mathcal{E}_{\mathbf{q}} - \mathcal{E}_{\mathbf{k}+\mathbf{q}}), \end{aligned} \quad (38)$$

where in the first line we have replaced  $V^{-1}\sum_{\mathbf{q}} = \int d^3\mathbf{q}/(2\pi)^3$ , and in the second line we have used (29), (33), and (34). We have also used the fact that  $F$  is Hermitian,  $F^{ud} = F^{du}$ , and the shorthand notation  $F_{\mathbf{q}} \equiv F(\mathbf{q})$ . Similarly, the right diagram in Fig. 2(b) corresponds to

$$i\Sigma_{\text{R}}^{Kdu}(p) = g^2 \int \frac{d^3\mathbf{q}}{(2\pi)^2} M_{\mathbf{q},\mathbf{k}-\mathbf{q}}^2 F_{\mathbf{q}}^{du} F_{\mathbf{k}-\mathbf{q}}^{du} \delta(\omega - \mathcal{E}_{\mathbf{q}} - \mathcal{E}_{\mathbf{k}-\mathbf{q}}), \quad (39)$$

where one needs to take a symmetry factor 2 into account. The total off-diagonal self-energy is then  $\Sigma^{Kdu} = \Sigma_{\text{L}}^{Kdu} + \Sigma_{\text{R}}^{Kdu}$ .

Calculating other components of  $\Sigma$  in a similar way, we get the collision integral (37) at leading order:

$$\begin{aligned} \text{St}_{\mathbf{k}}^{ud} & = g^2 \int \frac{d^3\mathbf{q}}{(2\pi)^2} \{ M_{\mathbf{q},\mathbf{k}-\mathbf{q}}^2 \delta(\mathcal{E}_{\mathbf{k}} - \mathcal{E}_{\mathbf{q}} - \mathcal{E}_{\mathbf{k}-\mathbf{q}}) [F_{\mathbf{q}}^{du} F_{\mathbf{k}-\mathbf{q}}^{du} - (F_{\mathbf{q}}^{uu} + F_{\mathbf{k}-\mathbf{q}}^{uu}) F_{\mathbf{k}}^{du}] \\ & + 2M_{\mathbf{k},\mathbf{q}}^2 \delta(\mathcal{E}_{\mathbf{k}} + \mathcal{E}_{\mathbf{q}} - \mathcal{E}_{\mathbf{k}+\mathbf{q}}) [F_{\mathbf{q}}^{du} F_{\mathbf{k}+\mathbf{q}}^{du} - (F_{\mathbf{q}}^{uu} - F_{\mathbf{k}+\mathbf{q}}^{uu}) F_{\mathbf{k}}^{du}] \}, \end{aligned} \quad (40)$$

$$\begin{aligned} \text{St}_{\mathbf{k}}^{uu} & = g^2 \int \frac{d^3\mathbf{q}}{(2\pi)^2} \{ M_{\mathbf{q},\mathbf{k}-\mathbf{q}}^2 \delta(\mathcal{E}_{\mathbf{k}} - \mathcal{E}_{\mathbf{q}} - \mathcal{E}_{\mathbf{k}-\mathbf{q}}) [F_{\mathbf{q}}^{uu} F_{\mathbf{k}-\mathbf{q}}^{uu} + 1 - (F_{\mathbf{q}}^{uu} + F_{\mathbf{k}-\mathbf{q}}^{uu}) F_{\mathbf{k}}^{uu}] \\ & + 2M_{\mathbf{k},\mathbf{q}}^2 \delta(\mathcal{E}_{\mathbf{k}} + \mathcal{E}_{\mathbf{q}} - \mathcal{E}_{\mathbf{k}+\mathbf{q}}) [F_{\mathbf{q}}^{uu} F_{\mathbf{k}+\mathbf{q}}^{uu} - 1 - (F_{\mathbf{q}}^{uu} - F_{\mathbf{k}+\mathbf{q}}^{uu}) F_{\mathbf{k}}^{uu}] \}. \end{aligned} \quad (41)$$

On the other hand,  $\text{St}^{du}$  and  $\text{St}^{dd}$  are simply related by  $u \leftrightarrow d$  symmetry. A crucial observation is that the diagonal  $\text{St}^{uu}$  is just the collision integral for TOC of subsystem  $u$ , which does not involve the off-diagonal  $F^{ud}$ . The reason is the two subsystems  $u$  and  $d$  evolve independently in time, and they are correlated only from the initial state  $\rho_c$ . As a consequence, when the operator  $\tilde{\mathcal{O}}$  perturbs the system away from the unperturbed equilibrium (23) and (24),  $F^{\kappa\kappa'} = F_0^{\kappa\kappa'} + \delta F^{\kappa\kappa'}$  where  $F_0^{uu} = F_0^{dd} = F_0$ , there are two classes of eigenmodes for  $\delta F^{\kappa\kappa'}$  as the solutions for the GBE (35). In the first class, both the diagonal and off-diagonal components of  $\delta F$  are nonvanishing, and the diagonal ones evolve independently according to (41). Since the perturbation is from the stable equilibrium (23), perturbations of this class are generally decaying modes  $\delta F^{\kappa\kappa'}(t) \propto e^{\lambda t}$  with  $\lambda < 0$ , so that the system returns to equilibrium at long time, guaranteed by the Boltzmann  $H$  theorem. In the second class, the diagonal ones vanish  $\delta F^{uu} = \delta F^{dd} = 0$ , and the off-diagonal  $\delta F^{du} \sim e^{\lambda t}$ , where now the  $\lambda$  is no longer guaranteed to be negative. If there is some eigenmode with  $\lambda > 0$ , it dominates at long times when the first class eigenmodes can be ignored. Therefore, to extract the Lyapunov exponent and butterfly velocity, it suffices to focus on the off-diagonal component of the GBE (35), with collision integral (40), where the diagonal distributions  $F^{uu} = F^{dd} = F_0$  are set to equilibrium (23).

We have established the GBE describing OTOC dynamics for the effective Hamiltonian (10), which comes from the original Bose gas Hamiltonian (6) via the Bogoliubov approximation (9). We now justify this approach in our nonequilibrium context. According to the previous paragraph, we are interested in the timescale long enough so that the two subsystems  $u$  and  $d$  have been in equilibrium, as probed locally in each subsystem. Similar to  $\delta F^{uu}$  that has already decayed at this timescale, whatever perturbations to the condensate of each subsystem caused by  $\tilde{\mathcal{O}}$  have also died out, so that (9) holds. Note that we also require this timescale is not too long, so that the intersubsystem probe  $\delta F^{du}$  has not grown beyond the linear regime. We also mention that we have discarded off-shell terms in (10c). This approximation is also legitimate, because the collision integral, (40) for example, involves only on-shell processes at leading order.

#### IV. LYAPUNOV EXPONENT

Since the Lyapunov exponent  $\lambda_L$  characterizes local scrambling, we can assume the perturbation is homogeneous  $F(x, \mathbf{k}) = F_{\mathbf{k}}(t)$  in space  $\mathbf{x}$ . Assuming  $F^{du} = F_0^{du} + \delta F^{du}$  and expanding (40) to linear order in  $\delta F^{du}$ , (35)

becomes

$$\begin{aligned}
 \partial_t \delta F_k^{du} &= 2 \frac{g^2}{\hbar} \int \frac{d^3 \mathbf{q}}{(2\pi)^2} \{ M_{q,k-q}^2 \delta(\mathcal{E}_k - \mathcal{E}_q - \mathcal{E}_{k-q}) [F_0^{du}(\mathcal{E}_{k-q}) \delta F_q^{du} - F_0(\mathcal{E}_q) \delta F_k^{du}] + M_{k,q}^2 \delta(\mathcal{E}_k + \mathcal{E}_q - \mathcal{E}_{k+q}) \\
 &\quad \times [F_0^{du}(\mathcal{E}_q) \delta F_{k+q}^{du} + F_0^{du}(\mathcal{E}_{k+q}) \delta F_q^{du} - (F_0(\mathcal{E}_q) - F_0(\mathcal{E}_{k+q})) \delta F_k^{du}] \}, \\
 &= \frac{8}{\hbar} \sqrt{na_s^3} \sqrt{TT_*} \int \frac{d^3 \tilde{\mathbf{q}}}{\sqrt{2\pi}} \{ \tilde{M}_{\tilde{q},\tilde{k}-\tilde{q}}^2 \delta(\tilde{\mathcal{E}}_k - \tilde{\mathcal{E}}_{\tilde{q}} - \tilde{\mathcal{E}}_{\tilde{k}-\tilde{q}}) [(\sinh \tilde{\mathcal{E}}_{\tilde{k}-\tilde{q}})^{-1} \delta F_{\tilde{q}}^{du} - \coth \tilde{\mathcal{E}}_{\tilde{q}} \delta F_{\tilde{k}}^{du}] + \tilde{M}_{\tilde{k},\tilde{q}}^2 \delta(\tilde{\mathcal{E}}_k + \tilde{\mathcal{E}}_{\tilde{q}} - \tilde{\mathcal{E}}_{\tilde{k}+\tilde{q}}) \\
 &\quad \times [(\sinh \tilde{\mathcal{E}}_{\tilde{q}})^{-1} \delta F_{\tilde{k}+\tilde{q}}^{du} + (\sinh \tilde{\mathcal{E}}_{\tilde{k}+\tilde{q}})^{-1} \delta F_{\tilde{q}}^{du} - (\coth \tilde{\mathcal{E}}_{\tilde{q}} - \coth \tilde{\mathcal{E}}_{\tilde{k}+\tilde{q}}) \delta F_{\tilde{k}}^{du}] \} \\
 &\equiv \sum_{\tilde{q}} \mathcal{M}_{\tilde{k},\tilde{q}} \delta F_{\tilde{q}}^{du}, \tag{42}
 \end{aligned}$$

where we have used the rescaled dimensionless parameters

$$\tilde{\mathbf{k}} = \frac{\hbar \mathbf{k}}{\sqrt{2mT}}, \quad \tilde{\mathcal{E}} = \frac{\mathcal{E}}{2T}, \quad \tilde{M} = M/\sqrt{n}. \tag{43}$$

The Lyapunov exponent is then the largest positive eigenvalue  $\max \text{eig}(\mathcal{M})$  of the matrix  $\mathcal{M}$ . Since  $\tilde{M}$  and  $\tilde{\mathcal{E}}$  in (42) only depends on  $T/T_*$ , we have the general form

$$\lambda_L = \hbar^{-1} \sqrt{na_s^3 T_*} f(T/T_*), \tag{44}$$

with  $f(\cdot)$  being a universal function. We further assume the mode corresponding to  $\lambda_L$  is isotropic:  $\delta F_k(t) = \delta F_k(t)$  with  $k \equiv |\mathbf{k}|$ , so that (42) reduces to  $\partial_t \delta F_k = \sum_{k'} \tilde{\mathcal{M}}_{k,k'} \delta F_{k'}$ , with details given in the Appendix on how to transform the integration measure. We take discrete values of  $k$  up to a cutoff  $k_{\text{cut}}$  to generate the  $\mathcal{M}$  matrix. The cutoff  $k_{\text{cut}}$  is much larger than  $k_0$ , such that the largest eigenvalues of  $\mathcal{M}$  are approximately independent of  $k_{\text{cut}}$ . Using the expression (13) for  $M_{k,q}$ , we then numerically solve for  $\lambda_L = \max \text{eig}(\tilde{\mathcal{M}})$  as a function of  $T$ , as shown in Fig. 3(a).

At sufficiently low temperature  $T \ll T_*$ , the quasiparticles are typically phonon-like  $\mathcal{E}_k \approx \hbar ck$  for  $k \ll k_0$ . In this regime the collision matrix  $M_{k_1,k_2} \approx 3 \left( \frac{nk_1 k_2 k_3}{27 k_0^3} \right)^{1/2}$  [52], so that the dependence of the matrix  $\tilde{\mathcal{M}}_{k,q}$  on  $T/T_*$  can be extracted as a prefactor proportional to  $T^5$ . From numerics, we indeed get

$$\lambda_L(T \ll T_*) \approx 761 \hbar^{-1} \sqrt{na_s^3 T_*} \left( \frac{T}{T_*} \right)^5, \tag{45}$$

as indicated by the red dashed line in Fig. 3(a). Equation (45) agrees *quantitatively* with the result on the unitary Fermi gas at low temperature that has a similar effective boson model [50], validating our calculation. The  $T^5$  scaling is parametrically smaller than the chaos bound [7]. Because the GBE shares similar forms with traditional Boltzmann equations that govern damping of quasiparticles, one expect they have the same timescales. Indeed, (45) is of the same order as the Belieav damping rate  $\frac{1}{\tau(k)} \sim \frac{k^5}{\hbar^3 mn}$  [55] evaluated at the typical phonon momentum  $k \approx T/\hbar c$ .

At relatively high temperature  $T \gg T_*$ , one can assume that all  $k$  of interest are in the particle regime  $k \sim \lambda_T^{-1} \gg k_0$  so that  $M_{k_1,k_2} \approx \sqrt{n}$ , and count the dimensions similarly. However, this naive dimension counting results in  $\lambda_L \propto \sqrt{T}$ , which disagrees with the numerical result

$$\lambda_L(T \gg T_*) \approx 4 \hbar^{-1} \sqrt{na_s^3 T}. \tag{46}$$

To resolve this issue, we plot the eigenmode  $\delta F_k^{du}$  that corresponds to the eigenvalue  $\lambda_L$  in Fig. 3(b), where the low temperature case is also included. For the blue line  $T/T_* = 10^3$ , We find that, although the  $k$  distribution  $k^2 \delta F_k^{du}$  sits largely in the  $k \sim \lambda_T^{-1}$  regime, it peaks at  $k \sim k_0$  instead. Thus the  $k \lesssim k_0$  momenta also contribute nontrivially to  $\lambda_T$ , resulting in the failure of the naive dimension counting argument. Comparing (46) to the Landau damping rate  $\frac{1}{\tau(k)} \sim \mathcal{E}_k \frac{dT}{\hbar c}$  at this temperature region [56,57], we find agreement  $\lambda_L \sim \frac{1}{\tau(k)}$  only for the peak value  $k \sim k_0$ , instead of the typical one  $k \sim \lambda_T^{-1}$ . This shows an interesting phenomenon where information is mostly scrambled by the small fraction of low-energy quasiparticles. The linear  $T$  behavior in (46) mimics models with holographic duals [11,12], although here the small prefactor  $(na_s^3)^{1/2} \ll 1$  means our theory is weakly interacting, and  $\lambda_L$  is still parametrically smaller than the chaos bound [7].

## V. BUTTERFLY VELOCITY

To further calculate the butterfly velocity  $v_B$ , we take the ansatz  $\delta F^{du}(\mathbf{x}) \propto e^{-i\ell \cdot \mathbf{x}}$  instead of the homogeneous one. Then the linearized GBE becomes

$$\partial_t \delta F_{\tilde{\mathbf{k}}}^{du} = \sum_{\tilde{\mathbf{q}}} (\mathcal{M} + i\ell \cdot \mathbf{v})_{\tilde{\mathbf{k}},\tilde{\mathbf{q}}} \delta F_{\tilde{\mathbf{q}}}^{du}, \tag{47}$$

with  $\mathcal{M}$  the same as (42), and the diagonal matrix

$$\mathbf{v}_{\tilde{\mathbf{k}},\tilde{\mathbf{q}}} = \mathbf{v}_k \delta_{\tilde{\mathbf{k}},\tilde{\mathbf{q}}}, \quad \text{where } \mathbf{v}_k = \nabla_k \mathcal{E}_k / \hbar. \tag{48}$$

The maximum eigenvalue  $\max \text{eig}(M + i\ell \cdot \mathbf{v})$  is then the Lyapunov exponent  $\lambda_L(\ell)$  at wave vector  $\ell$ , and the general solution takes the form  $\delta F^{du} \sim \int d\ell \chi_\ell e^{\lambda_L(\ell)t - i\ell \cdot \mathbf{x}}$ . Suppose the initial perturbation varies slowly in space, so that we can expand at small  $\ell$ :

$$\lambda_L(\ell) \approx \lambda_0 - \lambda_2 \ell^2 \pm i\lambda_1 \ell, \tag{49}$$

where  $\lambda_j$  are all non-negative. We then integrate over  $\ell$  by using the saddle-point approximation, by finding  $\ell$  that satisfies

$$\partial_\ell (\lambda_L(\ell) - i\ell \cdot \mathbf{x}) = 0, \tag{50}$$

$$\partial_\theta (\lambda_L(\ell) - i\ell \cdot \mathbf{x}) = 0, \tag{51}$$

<sup>1</sup>Since  $\delta F_k^{du}$  represents a density in  $k$  space and the system is isotropic,  $k^2 \delta F_k^{du}$  represents the density of  $k$  with all angular directions being integrated.

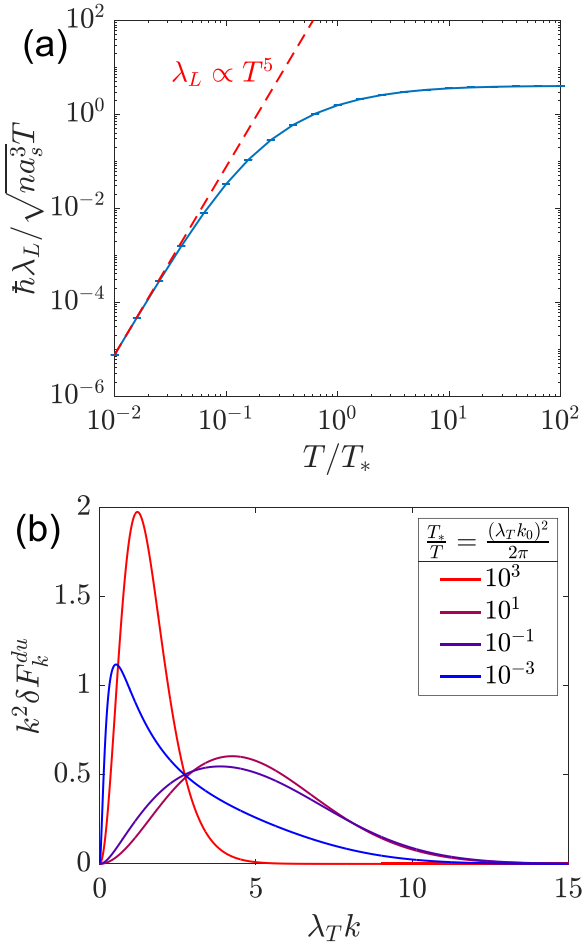


FIG. 3. (a) Blue solid line: Lyapunov exponent  $\lambda_L$  as a function of temperature  $T$ . The y axis is normalized to indicate the behavior  $\lambda_L \propto T$  at  $T \gg T_*$ , while the  $T \ll T_*$  behavior (45) is plotted in the red dashed line. Here we took a cutoff  $\tilde{k}_{\text{cut}} \lesssim 10$  in (42) and discretized to  $n_{\text{cut}} = 4000$  points of  $\tilde{k} \leq \tilde{k}_{\text{cut}}$ . We also computed the data when  $\tilde{k}_{\text{cut}}$  and  $n_{\text{cut}}$  are cut in half to estimate the error bar. The value of  $\tilde{k}_{\text{cut}}$  is optimized for each  $T$ , so that the error bar is barely visible. (b) The Lyapunov eigenmode  $\delta F_k^{du}$  as a function of  $k$ , at five temperatures shown in the legend. The amplitude of each mode is normalized so that  $\int dk k^2 \delta F_k^{du} = 1$ . A crucial observation is that  $k^2 \delta F_k^{du}$  peaks at  $k \sim k_0$  for  $T \gg T_*$ .

where  $\theta$  is the angle between  $\ell$  and  $\mathbf{x}$ . This gives

$$\delta F^{du} \sim \exp \left[ \lambda_0 t - \frac{(|\mathbf{x}| - \lambda_1 t)^2}{4\lambda_2 t} \right], \quad (52)$$

which decays exponentially for  $|\mathbf{x}| > v_B t$ , where

$$v_B = \lambda_1 + 2\sqrt{\lambda_0 \lambda_2} \equiv c \tilde{f}(T/T_*), \quad (53)$$

for some universal function  $\tilde{f}(\cdot)$ .

We numerically calculate  $\lambda_j$  by diagonalizing  $M + i\ell \cdot \mathbf{v}$ , and get  $v_B/c$  as a function of  $T/T_*$  in Fig. 4. Following the dimension-counting arguments in the previous section, at very low temperature  $T \ll T_*$ ,  $v_B$  is several times of the sound velocity  $c$ , the only velocity scale present in the system. Figure 4 suggests

$$v_B(T \ll T_*) \approx 4c. \quad (54)$$

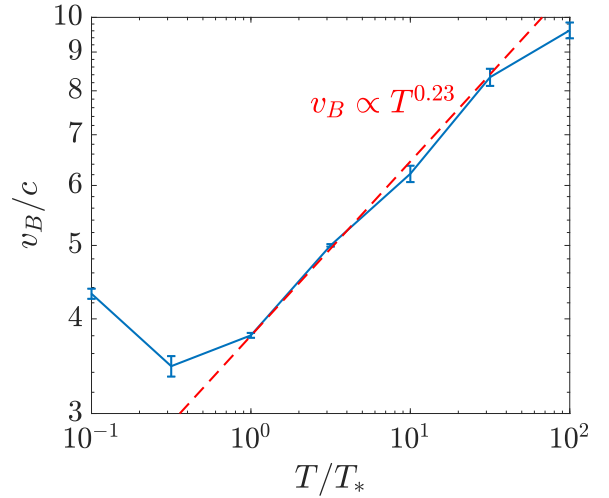


FIG. 4. Butterfly velocity  $v_B$  as a function of  $T$  shown by blue solid line, while the red dashed line represents (55). We assume rotational symmetry along  $z$  axis that  $\ell$  points, and diagonalize (47) in the  $(\tilde{k}_x = \tilde{k} \sin \theta_{\tilde{k}}, \tilde{k}_z = \tilde{k} \cos \theta_{\tilde{k}})$  plane using (A9) as the integration measure. We choose the region  $0 \leq \tilde{k}_x \leq \tilde{k}_{\text{cut}}, -\tilde{k}_{\text{cut}} \leq \tilde{k}_z \leq \tilde{k}_{\text{cut}}$ , with the cutoff  $\tilde{k}_{\text{cut}} \lesssim 4.5$  optimized for each  $T$ . This two-dimensional region is discretized to  $n_{\text{cut}} = 45000$  points, and we also computed the data when  $\tilde{k}_{\text{cut}}$  and  $n_{\text{cut}}$  are decreased by a factor of 4/5, to obtain the error bar.

However, the numerical factor 4 may be modified at temperature lower than  $0.1T_*$ , where our numerical algorithm yields fluctuating results and is thus not reliable. The more interesting region is at relatively high temperature  $T \gg T_*$ , where simple dimension counting fails. In Fig. 4, we observe a power-law dependence

$$v_B(T \gg T_*) \approx 3.8c \left( \frac{T}{T_*} \right)^{0.23}, \quad (55)$$

which is parametrically smaller than the typical velocity  $\sqrt{2T/m}$  of quasiparticles. This should be related to the anomalous clustering of the distribution  $\delta F_k^{du}$  at small  $k \approx k_0$  in Fig. 3(b), and demands further understanding. Surprisingly, the exponent 0.23 matches the one for the butterfly velocity in a classical spin chain [58], which suggests that drastically different microscopic models, may share universal behavior regarding information scrambling dynamics.

Using the values of  $\lambda_L$  and  $v_B$ , we calculate the quantity

$$D_L = v_B^2 / \lambda_L \sim \frac{\hbar}{m\sqrt{na^3}} \times \begin{cases} \left(\frac{T_*}{T}\right)^5, & T \ll T_* \\ \left(\frac{T_*}{T}\right)^{0.54}, & T \gg T_* \end{cases} \quad (56)$$

In certain strongly interacting models [27,59,60], such a chaos diffusion constant is found to agree with charge [21,26] and energy [27] diffusion constants. However, the model we study here is weakly interacting, and one does not expect  $D_L$  is related to the energy diffusion constant  $D_E = \kappa/c_v$  [61,62]. Indeed, using the formulas for heat conductivity  $\kappa$  [63,64] and heat capacity  $c_v$  [65], we get  $D_E$  for the dilute Bose gas:

$$D_E \sim \frac{\hbar}{m\sqrt{na^3}} \times \begin{cases} \frac{T_*}{T}, & T \ll T_* \\ \sqrt{\frac{T}{T_*}}, & T \gg T_* \end{cases} \quad (57)$$



TABLE I. Scaling laws of physical quantities describing chaos and energy diffusion, in the two temperature regimes.

| Physical quantity       | $T \ll T_*$   | $T \gg T_*$  |
|-------------------------|---|--|
| $\lambda_L$             | $\hbar^{-1} \sqrt{na_s^3} T_* \left(\frac{T}{T_*}\right)^5$ | $\hbar^{-1} \sqrt{na_s^3} T$                                     |
| $v_B$                   | $c$   | $c \left(\frac{T}{T_*}\right)^{0.23}$                            |
| $D_L = v_B^2/\lambda_L$ | $\frac{\hbar}{m\sqrt{na_s^3}} \left(\frac{T_*}{T}\right)^5$ | $\frac{\hbar}{m\sqrt{na_s^3}} \left(\frac{T_*}{T}\right)^{0.54}$ |
| $D_E = \kappa/c_v$      | $\frac{\hbar}{m\sqrt{na_s^3}} \frac{T_*}{T}$                | $\frac{\hbar}{m\sqrt{na_s^3}} \sqrt{\frac{T}{T_*}}$              |

which is not equal to  $D_L$ . Remarkably, both possibilities  $D_E \ll D_L$  and  $D_E \gg D_L$  arise, at very low and relatively high temperatures, respectively.

## VI. CONCLUSION

In this paper, we have calculated the quantum Lyapunov exponent  $\lambda_L$  and butterfly velocity  $v_B$  of the dilute Bose gas in the BEC phase, with results summarized in Table I. We find  $\lambda_L \propto T^5$  at very low temperature  $T \ll T_*$  and  $\lambda_L \propto T$  at relatively high temperature  $T_* \ll T \ll T_{\text{BEC}}$ . Meanwhile, we find  $v_B$  is at the order of the sound speed  $c$  at very low temperature, and follows a  $T^{0.23}$  power law at relatively high temperature. We have compared  $\lambda_L$  with the quasiparticle damping rate, and the chaos diffusion constant  $D_L = v_B^2/\lambda_L$  with the energy diffusion constant  $D_E$ . The weakly interacting nature of the model is manifested by the asymptotic smallness of  $\lambda_L$  compared with the chaos bound, and the mismatch between  $D_L$  and  $D_E$ . Our GBE method is proved to be efficient for calculating OTOC, since only two-point functions are involved. Experimental tests of our predictions would require either approaches to measure OTOC directly [66,67], or phenomenological connections between information scrambling and time-ordered physics. On the other hand, we expect our results can be generalized to higher temperature  $T \sim T_{\text{BEC}}$ , where fluctuation of the condensate and vortices become important [68].

## ACKNOWLEDGMENTS

We thank Pengfei Zhang and Andrew Lucas for useful discussions. Y.C. is supported by Beijing Natural Science Foundation (Z180013), and NSFC under Grants No. 12174358 and No. 11734010.

## APPENDIX: INTEGRATION MEASURE WITH SPHERICAL OR AXIAL SYMMETRY

We work with the dimensionless momentum  $\tilde{\mathbf{k}}$  defined in (43). First, assume  $\delta F_{\tilde{\mathbf{k}}}^{du} = \delta F_{\tilde{\mathbf{k}}}^{du}$  has spherical symmetry SO(3). Using  $(\tilde{q}, \theta, \varphi)$  as the spherical coordinate of  $\tilde{\mathbf{q}}$  with the polar axis pointing along  $\tilde{\mathbf{k}}$ , the integration measure in (42) becomes

$$\begin{aligned} \mathcal{I} &\equiv \int \frac{d^3\tilde{\mathbf{q}}}{\sqrt{2\pi}} \delta(\tilde{\mathcal{E}}_{\tilde{\mathbf{k}}} \mp \tilde{\mathcal{E}}_{\tilde{\mathbf{q}}} - \tilde{\mathcal{E}}_{\tilde{\mathbf{k}}\mp\tilde{\mathbf{q}}}) \\ &= \sqrt{2\pi} \int \tilde{q}^2 d\tilde{q} \sin\theta d\theta \frac{\delta(\theta - \theta^{\text{os}})}{|\partial_\theta \tilde{\mathcal{E}}_3|}, \end{aligned} \quad (\text{A1})$$

where  $\varphi$  has been integrated over,  $\tilde{\mathcal{E}}_3 \equiv \tilde{\mathcal{E}}_{\tilde{\mathbf{k}}\mp\tilde{\mathbf{q}}}$  is the energy of the third quasiparticle, and  $\theta^{\text{os}}$  is the polar angle such that the corresponding  $\tilde{\mathbf{q}}^{\text{os}}$  with length  $|\tilde{\mathbf{q}}^{\text{os}}| = \tilde{q}$  makes the three quasiparticles on-shell:  $\tilde{\mathcal{E}}_{\tilde{\mathbf{k}}} \mp \tilde{\mathcal{E}}_{\tilde{\mathbf{q}}^{\text{os}}} - \tilde{\mathcal{E}}_{\tilde{\mathbf{k}}\mp\tilde{\mathbf{q}}^{\text{os}}} = 0$ . To calculate the denominator in (A1), we use

$$\partial_\theta = (\partial_\theta \tilde{q}_3^2) \frac{d}{d\tilde{q}_3^2} = \pm \frac{\tilde{k}\tilde{q}}{\tilde{q}_3} \sin\theta \frac{d}{d\tilde{q}_3}, \quad (\text{A2})$$

because the momentum for the third quasiparticle is

$$\tilde{q}_3^2 = \tilde{k}^2 + \tilde{q}^2 \mp 2\tilde{k}\tilde{q} \cos\theta. \quad (\text{A3})$$

Then we integrate over  $\theta$  in (A1) to get the spherical symmetric integration measure

$$\mathcal{I} = \sqrt{2\pi} \int_0^\infty d\tilde{q} \frac{\tilde{q}_3 \tilde{q}}{\tilde{k} \left| \frac{d\tilde{\mathcal{E}}_3}{d\tilde{q}_3} \right|}, \quad (\text{A4})$$

where  $\tilde{q}_3(\tilde{k}, \tilde{q})$  is the on-shell momentum such that

$$\tilde{\mathcal{E}}_3(\tilde{q}_3) = \tilde{\mathcal{E}}_{\tilde{\mathbf{k}}} \mp \tilde{\mathcal{E}}_{\tilde{\mathbf{q}}}. \quad (\text{A5})$$

More generally, assume  $\delta F_{\tilde{\mathbf{k}}}^{du} = \delta F_{\tilde{\mathbf{k}}, \theta_{\tilde{\mathbf{k}}}}^{du}$  is not spherical symmetric, but still has the axial rotation symmetry SO(2) around the polar axis. In this case, assuming  $\tilde{\mathbf{k}}$  corresponds to  $\varphi_{\tilde{\mathbf{k}}} = 0$ , (A1) becomes

$$\mathcal{I} = \int \frac{\tilde{q}^2 d\tilde{q} \sin\theta d\theta}{\sqrt{2\pi}} \sum_j \frac{\delta(\varphi - \varphi_j^{\text{os}})}{|\partial_\varphi \tilde{\mathcal{E}}_3|}, \quad (\text{A6})$$

where there are either two or zero on-shell solutions for  $\varphi_j^{\text{os}}$ . The third momentum is now

$$\tilde{q}_3^2 = \tilde{k}^2 + \tilde{q}^2 \mp 2\tilde{k}\tilde{q}(\cos\theta_{\tilde{\mathbf{k}}} \cos\theta + \sin\theta_{\tilde{\mathbf{k}}} \sin\theta \cos\varphi), \quad (\text{A7})$$

so that

$$|\partial_\varphi \tilde{q}_3^2| = |2\tilde{k}\tilde{q} \sin\theta_{\tilde{\mathbf{k}}} \sin\theta \sin\varphi| = 2\tilde{k}\tilde{q} \left[ \sin^2\theta_{\tilde{\mathbf{k}}} \sin^2\theta - \left( \frac{\tilde{q}_3^2 - \tilde{k}^2 - \tilde{q}^2}{2\tilde{k}\tilde{q}} \pm \cos\theta_{\tilde{\mathbf{k}}} \cos\theta \right)^2 \right]^{1/2}. \quad (\text{A8})$$

Finally, we follow a similar strategy in (A2) to get

$$\mathcal{I} = 2 \int \frac{d\tilde{q} d\theta}{\sqrt{2\pi}} \frac{\tilde{q}_3 \tilde{q} \sin\theta}{\tilde{k} \left| \frac{d\tilde{\mathcal{E}}_3}{d\tilde{q}_3} \right|} \left[ \sin^2\theta_{\tilde{\mathbf{k}}} \sin^2\theta - \left( \frac{\tilde{q}_3^2 - \tilde{k}^2 - \tilde{q}^2}{2\tilde{k}\tilde{q}} \pm \cos\theta_{\tilde{\mathbf{k}}} \cos\theta \right)^2 \right]^{-1/2}, \quad (\text{A9})$$

where  $\tilde{q}_3$  is the on-shell solution for (A5).

- [1] A. Larkin and Y. N. Ovchinnikov, Quasiclassical method in the theory of superconductivity, *JETP* **28**, 960 (1969).
- [2] A. Kitaev, talk given at fundamental physics prize symposium, <http://online.kitp.ucsb.edu/online/joint98/kitaev/> (2014).
- [3] S. H. Shenker and D. Stanford, Black holes and the butterfly effect, *J. High Energy Phys.* **03** (2014) 067.
- [4] E. B. Rozenbaum, S. Ganeshan, and V. Galitski, Lyapunov Exponent and Out-of-Time-Ordered Correlator's Growth Rate in a Chaotic System, *Phys. Rev. Lett.* **118**, 086801 (2017).
- [5] T. Xu, T. Scaffidi, and X. Cao, Does Scrambling Equal Chaos? *Phys. Rev. Lett.* **124**, 140602 (2020).
- [6] C. Yin and A. Lucas, Quantum operator growth bounds for kicked tops and semiclassical spin chains, *Phys. Rev. A* **103**, 042414 (2021).
- [7] J. Maldacena, S. H. Shenker, and D. Stanford, A bound on chaos, *J. High Energy Phys.* **08** (2016) 106.
- [8] S. H. Shenker and D. Stanford, Multiple shocks, *J. High Energy Phys.* **12** (2014) 046.
- [9] S. H. Shenker and D. Stanford, Stringy effects in scrambling, *J. High Energy Phys.* **05** (2015) 132.
- [10] D. A. Roberts, D. Stanford, and L. Susskind, Localized shocks, *J. High Energy Phys.* **03** (2015) 051.
- [11] A. Kitaev, talk given at kitp program: Entanglement in strongly-correlated quantum matter, <http://online.kitp.ucsb.edu/online/entangled15/kitaev/> (2015).
- [12] J. Maldacena and D. Stanford, Remarks on the Sachdev-Ye-Kitaev model, *Phys. Rev. D* **94**, 106002 (2016).
- [13] J. Maldacena, D. Stanford, and Z. Yang, Conformal symmetry and its breaking in two-dimensional nearly anti-de Sitter space, *Prog. Theor. Exp. Phys.* **2016**, 12C104 (2016).
- [14] R. Jackiw, Lower dimensional gravity, *Nucl. Phys. B* **252**, 343 (1985).
- [15] C. Teitelboim, Gravitation and Hamiltonian structure in two spacetime dimensions, *Phys. Lett. B* **126**, 41 (1983).
- [16] N. Lashkari, D. Stanford, M. Hastings, T. Osborne, and P. Hayden, Towards the fast scrambling conjecture, *J. High Energy Phys.* **04** (2013) 022.
- [17] G. Bentsen, Y. Gu, and A. Lucas, Fast scrambling on sparse graphs, *Proc. Natl. Acad. Sci. U. S. A.* **116**, 6689 (2019).
- [18] C. Yin and A. Lucas, Bound on quantum scrambling with all-to-all interactions, *Phys. Rev. A* **102**, 022402 (2020).
- [19] P. Hosur, X.-L. Qi, D. A. Roberts, and B. Yoshida, Chaos in quantum channels, *J. High Energy Phys.* **02** (2016) 004.
- [20] D. A. Roberts and B. Swingle, Lieb-Robinson Bound and the Butterfly Effect in Quantum Field Theories, *Phys. Rev. Lett.* **117**, 091602 (2016).
- [21] M. Blake, Universal Charge Diffusion and the Butterfly Effect in Holographic Theories, *Phys. Rev. Lett.* **117**, 091601 (2016).
- [22] A. Lucas and J. Steinberg, Charge diffusion and the butterfly effect in striped holographic matter, *J. High Energy Phys.* **10** (2016) 143.
- [23] X. Han and S. A. Hartnoll, Quantum scrambling and state dependence of the butterfly velocity, *SciPost Phys.* **7**, 045 (2019).
- [24] C. Yin and A. Lucas, Finite Speed of Quantum Information in Models of Interacting Bosons at Finite Density, *Phys. Rev. X* **12**, 021039 (2022).
- [25] E. H. Lieb and D. W. Robinson, The finite group velocity of quantum spin systems, *Commun. Math. Phys.* **28**, 251 (1972).
- [26] M. Blake, Universal diffusion in incoherent black holes, *Phys. Rev. D* **94**, 086014 (2016).
- [27] A. A. Patel and S. Sachdev, Quantum chaos on a critical Fermi surface, *Proc. Natl. Acad. Sci. U. S. A.* **114**, 1844 (2017).
- [28] S. Xu and B. Swingle, Scrambling dynamics and out-of-time ordered correlators in quantum many-body systems: A tutorial, [arXiv:2202.07060](https://arxiv.org/abs/2202.07060).
- [29] Y. Huang, Y.-L. Zhang, and X. Chen, Out-of-time-ordered correlators in many-body localized systems, *Ann. Phys. (Berlin, Ger.)* **529**, 1600318 (2017).
- [30] R. Fan, P. Zhang, H. Shen, and H. Zhai, Out-of-time-order correlation for many-body localization, *Sci. Bull.* **62**, 707 (2017).
- [31] Y. Chen, Universal logarithmic scrambling in many body localization, [arXiv:1608.02765](https://arxiv.org/abs/1608.02765).
- [32] B. Swingle and D. Chowdhury, Slow scrambling in disordered quantum systems, *Phys. Rev. B* **95**, 060201(R) (2017).
- [33] R.-Q. He and Z.-Y. Lu, Characterizing many-body localization by out-of-time-ordered correlation, *Phys. Rev. B* **95**, 054201 (2017).
- [34] B. Dóra and R. Moessner, Out-of-Time-Ordered Density Correlators in Luttinger Liquids, *Phys. Rev. Lett.* **119**, 026802 (2017).
- [35] A. Bohrdt, C. B. Mendl, M. Endres, and M. Knap, Scrambling and thermalization in a diffusive quantum many-body system, *New J. Phys.* **19**, 063001 (2017).
- [36] A. A. Patel, D. Chowdhury, S. Sachdev, and B. Swingle, Quantum Butterfly Effect in Weakly Interacting Diffusive Metals, *Phys. Rev. X* **7**, 031047 (2017).
- [37] Y. Liao and V. Galitski, Nonlinear sigma model approach to many-body quantum chaos: Regularized and unregularized out-of-time-ordered correlators, *Phys. Rev. B* **98**, 205124 (2018).
- [38] J. Li, R. Fan, H. Wang, B. Ye, B. Zeng, H. Zhai, X. Peng, and J. Du, Measuring Out-of-Time-Order Correlators on a Nuclear Magnetic Resonance Quantum Simulator, *Phys. Rev. X* **7**, 031011 (2017).
- [39] K. X. Wei, P. Peng, O. Shtanko, I. Marvian, S. Lloyd, C. Ramanathan, and P. Cappellaro, Emergent Prethermalization Signatures in Out-of-Time Ordered Correlations, *Phys. Rev. Lett.* **123**, 090605 (2019).
- [40] X. Nie, B.-B. Wei, X. Chen, Z. Zhang, X. Zhao, C. Qiu, Y. Tian, Y. Ji, T. Xin, D. Lu, and J. Li, Experimental Observation of Equilibrium and Dynamical Quantum Phase Transitions via Out-of-Time-Ordered Correlators, *Phys. Rev. Lett.* **124**, 250601 (2020).
- [41] M. Gärtner, J. G. Bohnet, A. Safavi-Naini, M. L. Wall, J. J. Bollinger, and A. M. Rey, Measuring out-of-time-order correlations and multiple quantum spectra in a trapped ion quantum magnet, *Nat. Phys.* **13**, 781 (2017).
- [42] M. K. Joshi, A. Elben, B. Vermersch, T. Brydges, C. Maier, P. Zoller, R. Blatt, and C. F. Roos, Quantum Information Scrambling in a Trapped-Ion Quantum Simulator with Tunable Range Interactions, *Phys. Rev. Lett.* **124**, 240505 (2020).
- [43] M. S. Blok, V. V. Ramasesh, T. Schuster, K. O'Brien, J. M. Kreikebaum, D. Dahlen, A. Morvan, B. Yoshida, N. Y. Yao, and I. Siddiqi, Quantum Information Scrambling on a Superconducting Qutrit Processor, *Phys. Rev. X* **11**, 021010 (2021).
- [44] X. Mi, P. Roushan, C. Quintana, S. Mandra, J. Marshall, C. Neill, F. Arute, K. Arya, J. Atalaya, R. Babbush *et al.*, Information scrambling in quantum circuits, *Science* **374**, 1479 (2021).
- [45] J. Braumüller, A. H. Karamlou, Y. Yanay, B. Kannan, D. Kim, M. Kjaergaard, A. Melville, B. M. Niedzielski, Y. Sung, A. Vepsäläinen *et al.*, Probing quantum information propagation with out-of-time-ordered correlators, *Nat. Phys.* **18**, 172 (2022).

- [46] M. H. Anderson, J. R. Ensher, M. R. Matthews, C. E. Wieman, and E. A. Cornell, Observation of Bose-Einstein condensation in a dilute atomic vapor, *Science* **269**, 198 (1995).
- [47] I. L. Aleiner, L. Faoro, and L. B. Ioffe, Microscopic model of quantum butterfly effect: Out-of-time-order correlators and traveling combustion waves, *Ann. Phys. (NY)* **375**, 378 (2016).
- [48] M. J. Klug, M. S. Scheurer, and J. Schmalian, Hierarchy of information scrambling, thermalization, and hydrodynamic flow in graphene, *Phys. Rev. B* **98**, 045102 (2018).
- [49] S. Grozdanov, K. Schalm, and V. Scopelliti, Kinetic theory for classical and quantum many-body chaos, *Phys. Rev. E* **99**, 012206 (2019).
- [50] P. Zhang, Quantum chaos for the unitary Fermi gas from the generalized Boltzmann equations, *J. Phys. B: At., Mol. Opt. Phys.* **52**, 135301 (2019).
- [51] H. Zhai, *Ultracold Atomic Physics* (Cambridge University Press, 2021).
- [52] M. Imamovic-Tomasovic and A. Griffin, Quasiparticle kinetic equation in a trapped Bose gas at low temperatures, *J. Low Temp. Phys.* **122**, 617 (2001).
- [53] A. Romero-Bermúdez, K. Schalm, and V. Scopelliti, Regularization dependence of the OTOC. Which Lyapunov spectrum is the physical one? *J. High Energy Phys.* **07** (2019) 107.
- [54] A. Kamenev, *Field Theory of Non-Equilibrium Systems* (Cambridge University Press, 2011).
- [55] S. T. Beliaev, Energy spectrum of a non-ideal Bose gas, *Sov. Phys. JETP* **7**, 299 (1958).
- [56] P. Szépfalussy and I. Kondor, On the dynamics of continuous phase transitions, *Ann. Phys. (NY)* **82**, 1 (1974).
- [57] M.-C. Chung and A. B. Bhattacharjee, Damping in 2d and 3d dilute Bose gases, *New J. Phys.* **11**, 123012 (2009).
- [58] T. Bilitewski, S. Bhattacharjee, and R. Moessner, Temperature Dependence of the Butterfly Effect in a Classical Many-Body System, *Phys. Rev. Lett.* **121**, 250602 (2018).
- [59] Y. Gu, X.-L. Qi, and D. Stanford, Local criticality, diffusion and chaos in generalized Sachdev-Ye-Kitaev models, *J. High Energy Phys.* **05** (2017) 125.
- [60] R. A. Davison, W. Fu, A. Georges, Y. Gu, K. Jensen, and S. Sachdev, Thermoelectric transport in disordered metals without quasiparticles: The Sachdev-Ye-Kitaev models and holography, *Phys. Rev. B* **95**, 155131 (2017).
- [61] Y. Gu, A. Lucas, and X.-L. Qi, Energy diffusion and the butterfly effect in inhomogeneous Sachdev-Ye-Kitaev chains, *SciPost Phys.* **2**, 018 (2017).
- [62] Y. Werman, S. A. Kivelson, and E. Berg, Quantum chaos in an electron-phonon bad metal, [arXiv:1705.07895](https://arxiv.org/abs/1705.07895).
- [63] T. R. Kirkpatrick and J. R. Dorfman, Transport theory for a weakly interacting condensed Bose gas, *Phys. Rev. A* **28**, 2576 (1983).
- [64] T. R. Kirkpatrick and J. R. Dorfman, Transport coefficients in a dilute but condensed Bose gas, *J. Low Temp. Phys.* **58**, 399 (1985).
- [65] C. J. Pethick and H. Smith, *Bose-Einstein Condensation in Dilute Gases* (Cambridge University Press, 2008).
- [66] B. Swingle, G. Bentsen, M. Schleier-Smith, and P. Hayden, Measuring the scrambling of quantum information, *Phys. Rev. A* **94**, 040302(R) (2016).
- [67] B. Vermersch, A. Elben, L. M. Sieberer, N. Y. Yao, and P. Zoller, Probing Scrambling Using Statistical Correlations between Randomized Measurements, *Phys. Rev. X* **9**, 021061 (2019).
- [68] A. Griffin, T. Nikuni, and E. Zaremba, *Bose-Condensed Gases at Finite Temperatures* (Cambridge University Press, 2009).